

Macro Diversity Gain in UMTS Networks with Clustered User Distributions

K. Heck^a, D. Staehle^a, K. Leibnitz^a

^aDepartment of Distributed Systems, University of Würzburg,
Am Hubland, 97074 Würzburg, Germany

In this paper we investigate the impact of user distributions on the macro diversity gain in UMTS environments. Earlier studies indicated that macro diversity has a beneficial influence on the system capacity and coverage of WCDMA systems. However, these investigations were based on the assumption of evenly distributed traffic patterns. In practice rather clustered user distributions are experienced, thus, the study of uneven user distributions is of great importance to the planning of 3rd generation mobile networks. Using a Matern process to create clustered user point fields, the pair-correlation function is presented as a measure for this unevenness. Simulation studies are used to evaluate its impact on the macro-diversity gain in UMTS networks. Results prove the non-intuitive fact that the unevenness as found in reality helps to further improve the system capacity and coverage.

1. INTRODUCTION

In cellular Wideband Code Division Multiple Access (WCDMA) systems, such as the Universal Mobile Telecommunication System (UMTS), in-cell interference has long been identified as the limiting factor. It does not only restrict the number of users within a cell, but it also impacts the coverage area [12]. The fact that all mobile stations (MS) in WCDMA environments utilize the same frequency band results in additional interference caused by MSs in neighboring cells (other-cell interference) and leads to a degradation of a cell's capacity and coverage area.

On the other hand, using a unique frequency band allows simultaneous connections from a MS to several base stations (BS) in close vicinity (Active Set, AS) [5]. Thus, soft and softer handover become possible and can be used to reduce interference induced by the MSs. The usage of multiple radio links is frequently referred to as *macro diversity*. It is also known as the combination of *site diversity*, the data reception at multiple sites, and *selection diversity*, the method of choosing a packet from the multiple replicas received.

Various studies about the gain achievable by site/selection diversity can be found in the literature. In [6] the authors performed experiments to evaluate the influence of different selection combining (SC) mechanisms on the gain in terms of relative MS transmit power. The impact of soft handover on the capacity of a CDMA system was studied analytically in [4]. However, only a simple model consisting of two BSs and one MS was considered. A more elaborate model was presented in [7] and a tradeoff between the capacity and

the coverage in a cell with mobiles allowed to be in soft handover was presented. The influence of the cell layout on the gain achieved by macro-diversity was studied in [13] and a possible access network architecture was proposed.

In order to take the interdependencies between neighboring cells in a UMTS network into consideration larger scenarios have to be studied. These scenarios are usually populated with users by some spatial point process and analyzed thereafter. The most frequently used point process is the *homogeneous spatial Poisson process*. In [1] a network consisting of a number of BSs is considered and outage probabilities are calculated.

While there are several other publications using the homogenous spatial Poisson process, such as [11] or [8], only little research is performed using other less even user distributions. In [9] the authors studied the influence of uneven user distributions on the soft handover gain in UMTS environments. However, site and selection diversity were not taken into account, but only single connections were considered. However, it was shown that the soft handover gain achievable in unevenly distributed user scenarios exceeds the gain found using even user distributions. In practice rather clustered user distributions are experienced, thus, the study of uneven user distributions is of great importance to the planning of 3rd generation mobile networks.

In this article we extend the work of [3] to derive site/selection diversity effects on the soft handover gain achievable for uneven user distributions. The model will be explained in Section 2. The Matern cluster process used to populate the network scenarios will be discussed in Section 3 and the level of unevenness of this cluster process compared to the spatial homogeneous Poisson process will be studied. The results are shown and discussed in Section 4 while Section 5 provides a conclusion and an outlook.

2. ANALYTICAL MODEL

The analysis method to calculate the site/selection diversity gain was taken from [3] and will be shortly explained in the following.

The scenario under study is an area with hexagonal cell layout consisting of 39 BSs as depicted in Figure 1. The BSs are displayed as grey triangles and the cells are shown as hexagons. The distance between the base stations is set to be 2 km. In the original approach a *homogeneous spatial Poisson process* was used to randomly create users within this scenario as indicated by the black dots. The user density in the picture is set to $\lambda = 2$ which maps to an average of two users per square kilometer.

In UMTS networks, the interference within a cell (in-cell interference) is greatly influenced by the interference in its neighboring cells (other-cell interference). Thus, only cells with surrounding neighboring cells are taken into consideration for the calculation of the results. In our case only the inner seven cells, highlighted in the picture, are used.

A set of formulae to iteratively calculate the important characteristics of the given UMTS scenario was taken from [8]. The interference level within a given cell can be derived by

$$\hat{I}_l = \frac{1}{W} \sum_k \hat{S}_k \hat{d}_{k,l} \nu_k, \quad (1)$$

where \hat{S}_k and ν_k denote the transmission power and activity factor of MS k , respectively, $\hat{d}_{k,l}$ stands for the path loss of MS k to BS l , and W marks the system bandwidth in

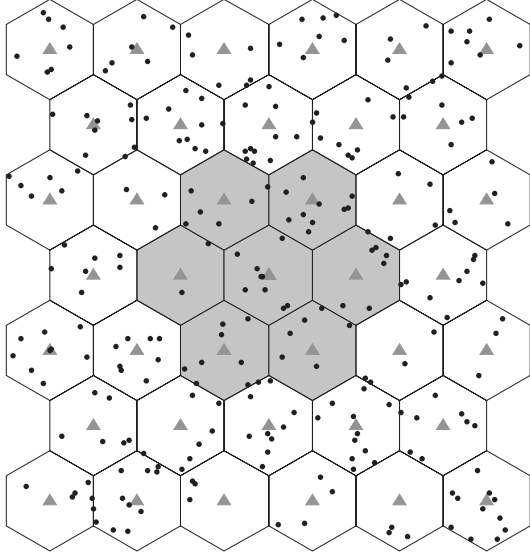


Figure 1. Snapshot of a homogeneous spatial Poisson process

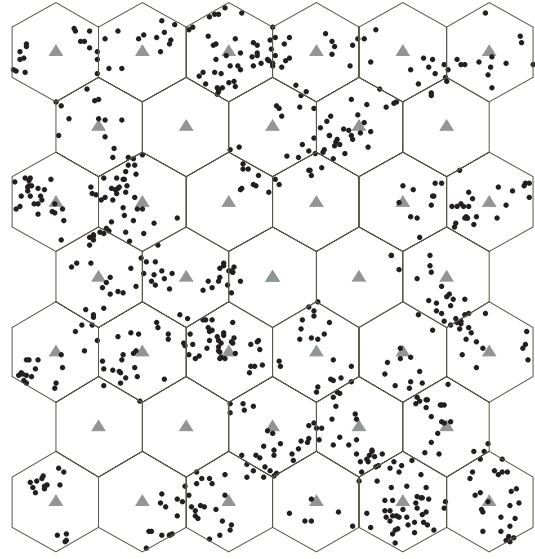


Figure 2. Snapshot of a Matern cluster process

Hertz. Here, for any variable X expressed in decibels (dB), \hat{X} denotes $10^{\frac{X}{10}}$. The power control equations (see e.g. [12])

$$\hat{c}_k^* = \frac{\frac{\hat{S}_k \hat{d}_{k,l}}{R_k}}{\hat{N}_0 + \hat{I}_l - \frac{\hat{S}_k \hat{d}_{k,l} \nu_k}{W}} \quad (2)$$

define a way to calculate the effective E_b/N_0 \hat{c}_k^* for each MS k . R_k denotes the bit rate of MS k and \hat{N}_0 specifies the background noise power spectral density. Solving Eq. (2) for \hat{S}_k yields

$$\hat{S}_k = \frac{W}{\hat{d}_{k,l}} (\hat{N}_0 + \hat{I}_l) \frac{\beta_k}{W + \beta_k \nu_k} \quad (3)$$

with $\beta_k = \hat{c}_k^* R_k$, an abbreviation for the product of bit rate and target E_b/N_0 of MS k .

Now, for each of the MSs in the given scenario, the initial target E_b/N_0 value can be specified depending on the data rate of the MS. Using Eq. (3) the initial transmission power \hat{S}_k necessary to reach this E_b/N_0 value at BS l can be calculated for each MS k and all BSs. In our case, we are only interested in the minimum transmission power for each MS k considering all BSs as possible receivers. In the next step, this minimum transmission power \hat{S}_k can be inserted in Eq. (2) to calculate the effective E_b/N_0 value of MS k at BS l .

As mentioned before, a single mobile in an UMTS environment is simultaneously connected to a set of BSs as specified by the Active Set (AS) of a MS. The AS only depends on the position of a MS within the given scenario and is derived using the relative strengths

of the received pilot signals as explained in [3]. Therefore, the effective E_b/N_0 value is calculated for all connections between a MS and the BSs in its Active Set.

Depending on these E_b/N_0 values, the bit error rate (BER) on the air interface can be calculated for each single connection by

$$p_b = Q(\sqrt{2\hat{\epsilon}_{k,l}}), \quad (4)$$

where the error function Q is given by

$$Q(x) = \frac{1}{\sqrt{2\pi}} \int_x^\infty e^{-\frac{x^2}{2}} dx. \quad (5)$$

In order to derive the frame error rate (FER) from the BER for 12.2 kbps voice users, the function

$$f(x) = \frac{\tanh(32 * x - 5)}{2} + \frac{\tanh(5)}{2} \quad (6)$$

was taken from [3], which proved to be a good approximation.

Assuming independent FERs for the different connections of a single MS, the overall FER of MS k can be derived by

$$FER_k = \prod_{k \in AS_k} (FER^{(k,l)}). \quad (7)$$

In UMTS environments power control mechanisms are used to adapt the target E_b/N_0 value of each MS in such a way that the FER_k is as close as possible to the target FER . Increasing the target E_b/N_0 results in a lower FER_k while decreasing the target E_b/N_0 yields a higher FER_k . In our analysis, the step size of the adaptation is chosen proportional to the difference between the actual and the target FER such that iterative convergence is reached.

After these adjustments, the next iteration can be started by recalculating Eq. (3) on the new target E_b/N_0 values. Ultimately, this algorithm leads to an iterative reduction of the interference within the cells and will thus converge to some minimum. Once all the actual FERs are less than 10^{-7} above or below the target FERs, the algorithm is considered to having reached the convergence and stops.

The case where no site/selection diversity is considered can be modeled exactly the same way with the only exception that the frame error rate FER_k is calculated by

$$FER_k = \min_{k \in AS_k} (FER^{(k,l)}). \quad (8)$$

Hence, only the connection to the BS with the least requirements is taken into account. Comparing the results obtained by the analysis using Eq. (8) and Eq. (7) yields the site/selection diversity gain.

The assumption of independent FER values for the different connections of a single MS does not hold in practice. Therefore, this approach is a best-case consideration and yields the maximum gain reachable with site/selection diversity.

3. CLUSTERED SPATIAL PROCESSES

Several publications can be found in the literature using homogeneous spatial Poisson processes for generating user fields within the analyzed scenarios, such as [11] and [8]. However, the user distributions found in practice are rather uneven, such that the Poisson process cannot reflect these scenarios.

Therefore, we will use a Matern process, a special type of a Neyman-Scott process, to generate clustered user fields. The Matern process employs a homogeneous spatial Poisson process with density λ_e to create the *parent points* which are used as the centers of the clusters. In the next step, the *daughter points* are generated in circles with radius R around each parent point. This is performed using another homogeneous spatial Poisson process with density μ . These daughter points will represent the users in our model.

An example of a resulting scenario is depicted in Figure 2 with parameters $\lambda_e = 1$, $R = 0.5$, and $\mu = 6$.

A Matern cluster field is still homogeneous by definition (see [10]). However, it is not as evenly distributed as the spatial homogeneous Poisson process. In order to measure the level of unevenness of the considered user distribution, the pair correlation function (pcf)

$$g(r) = \frac{\hat{\rho}(r)}{\lambda^2}; r \geq 0 \tag{9}$$

will be used, where $\hat{\rho}(r)$ defines the second-order intensity and λ is the first-order intensity, as described in [2].

From [10] we know an estimation for $\hat{\rho}$ with

$$\hat{\rho}(r) = \frac{1}{2\pi r} \sum_{i=1}^n \sum_{\substack{j=1 \\ (j \neq i)}}^n \frac{k_h(r - \|x_j - x_i\|)}{A(W_{x_j} \cap W_{x_i})}, \tag{10}$$

where

$$k_h(t) = \frac{3}{4h} \left(1 - \frac{t^2}{h^2}\right); \quad -h \leq t \leq h \tag{11}$$

and

$$h = 0.2 \sqrt{\frac{1}{\lambda_e \mu}}. \tag{12}$$

Figure 3 compares the pcf of a normal homogeneous spatial Poisson process to the pcf of a Matern cluster process with parameters $\lambda_e = 1$, $R = 1$, and $\mu = 3$. Both processes have the same density, that is

$$\lambda = \lambda_e \mu = 3,$$

such that the average number of users is equal for both processes. However, the distribution of the distance between two randomly chosen dots is different for the two processes, since the Matern cluster process produces clusters and short distances will occur more often.

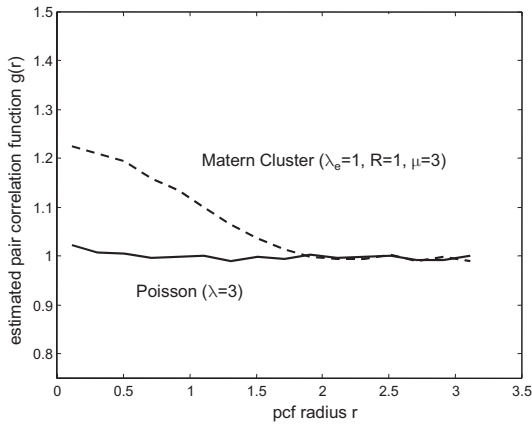


Figure 3. Estimated pair correlation functions

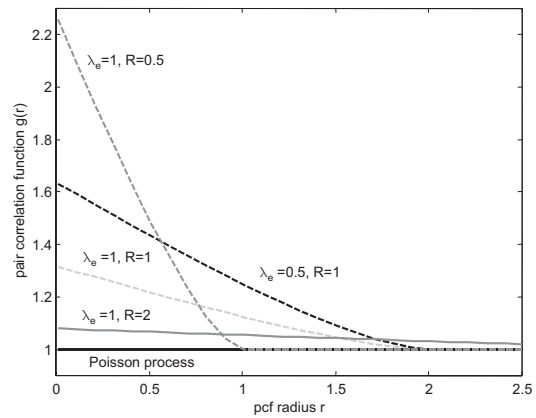


Figure 4. Comparison of the unevenness of Matern cluster processes

The pair correlation function uses this fact to measure the level of unevenness. For a given radius r , circles are placed around the dots within the given scenario and the number of dots within these circles is measured. The pcf then states the ratio between the average user density $\lambda_e \mu$ and the measured user density within the considered circles. For the spatial homogeneous Poisson process the ratio is 1 for all radii r since the points are evenly distributed in the whole area. Obviously, this does not hold for the Matern cluster process. Figure 3 shows that there are more users in close proximity than for the Poisson process. This is due to the clusters created by the Matern process.

Since the estimation is not correct for a finite area, a number of scenarios has been created and analyzed. The resulting pair correlation functions have been used to calculate the mean overall pair correlation function.

However, there is a way to calculate the pcf for the Matern cluster process. It has been derived in [10] as

$$g(r) = 1 + \frac{f(r)}{2\pi\lambda_e r}; \quad r \geq 0, \quad (13)$$

where

$$s(r) = \arccos \frac{r}{2R} - \frac{r}{2R} \sqrt{1 - \frac{r^2}{4R^2}}, \quad (14)$$

and

$$f(r) = \begin{cases} \frac{4rs(r)}{\pi R^2} & ; \quad 0 \leq r \leq 2R \\ 0 & ; \quad r > 2R \end{cases} \quad (15)$$

The equations show that the pcf of the Matern process is independent of the daughter point density μ . Figure 4 depicts the pair correlation functions for various values of λ_e and radii R .

Comparing the three curves for parent point density $\lambda_e = 1$ exhibits two distinct effects of varying the cluster size $R = 0.5, 1, 2$ on the pair correlation function.

The first effect is that for larger clusters R the pair correlation function of the related point field coincides with the Poisson case only for higher values of r , that is the two curves coincide for the case that

$$r \geq 2R. \quad (16)$$

In other words, the unevenness of the Matern cluster process is limited to the circle of two times the cluster size around the created points. Let λ_p define the density of points within a given circle around some point. Now, if the circle is larger than two times the cluster size, the number of points within this area matches the density of the overall Matern cluster field, that is

$$\lambda_p = \lambda_e \mu, \quad (17)$$

while circles of smaller size show larger densities of points, i.e.

$$\lambda_p > \lambda_e \mu. \quad (18)$$

The second effect is that small Matern clusters lead to higher *local unevenness*, which means that the pair correlation function $g(r)$ of the Matern cluster fields increases with diminishing radius R . The term *local* refers to small values of r . In other words, when considering a small circle around some point of the Matern cluster field, the density of points within this circle λ_p , will be higher for smaller Matern clusters R .

On the other hand, Figure 4 also shows the effect of varying the density of the parent points λ_e . The value r for which the pair correlation functions coincide with the pcf of the Poisson field stays the same. However, the unevenness increases for smaller densities, e.g. in the case $r = 1$, the Matern cluster field ($\lambda_e = 1, R = 1$) has the pcf value $g(r) = 1.1245$ while in the case of ($\lambda_e = 0.5, R = 1$) the pcf value is $g(r) = 1.2489$, which means that the unevenness of the Matern cluster process increases for smaller parent point densities.

We can conclude that varying the parent point density λ_e of a Matern cluster process will increase the unevenness of the resulting cluster fields. The point fields can be directly compared to one another in terms of their unevenness.

However, changing the cluster size R has a different effect. The local unevenness (within small areas around the points) increases for smaller clusters, but is restricted to an area of two times the cluster size around any point. This means, that larger clusters exhibit an unevenness in larger areas. However, the unevenness of the resulting cluster fields can not as easily be compared to one another.

In the next Section, the influence of the unevenness of various Matern cluster processes on the site/selection diversity gain will be examined.

4. RESULTS

Simulations of 39 cell area were performed to calculate the results. Within this area different Matern cluster processes were used to create random 12.2 kbps voice users. For each of these scenarios the site/selection diversity was calculated and will be compared to the results found by using the spatial homogeneous Poisson process. The simulation

has to be repeated for a number of user point fields in order to retrieve a certain level of stochastic relevance which is indicated by the 90% confidence interval in all the presented plots.

The site/selection diversity gain can be stated by different measures. One way is to use the mean interference reduction within the seven inner cells (see Section 2). This is used in Figure 5, where the abscissa specifies the user density of the point field (λ for Poisson and $\lambda_e\mu$ for Matern) and the ordinate shows the mean interference reduction in decibels.

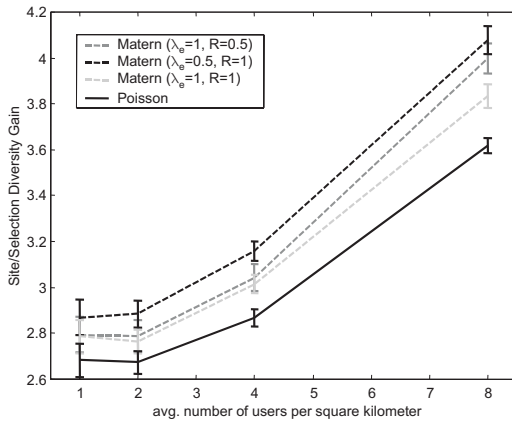


Figure 5. Soft Handover Gain as interference reduction

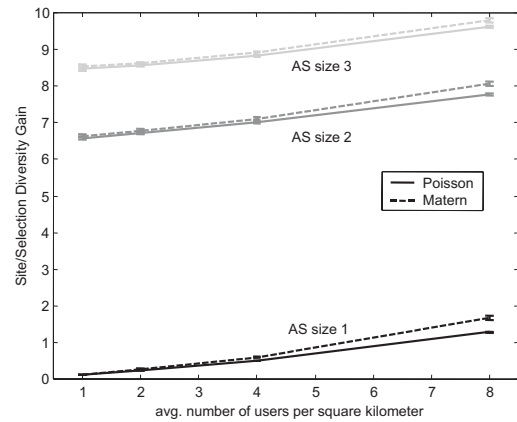


Figure 6. Transmit power reduction depending on AS sizes

The results for the Poisson case can also be found in [3]. As explained in the last Section, the unevenness of the cluster point fields created by a Matern process with varying parent point density λ_e can be directly compared to each other. Thus, we can derive that the curve for $(\lambda_e = 0.5, R = 1)$ reflects a higher unevenness than the curve for $(\lambda_e = 1, R = 1)$. This is directly related to the results shown in Figure 5.

Both curves state an increase of site/selection diversity gain, while the increase in unevenness leads to larger gains. The run of the curves is almost identical but only shifted on the ordinate based on the level of unevenness. The observable increase in site/selection diversity gain ranges from 0.10 to 0.21 dB for $\lambda_e = 1$ and from 0.19 to 0.46 dB for $\lambda_e = 0.5$. We can conclude that the additional gain caused by unevenness increases proportionally to the level of unevenness in the case of varying parent point density λ_e .

On the other hand, the curve for $(\lambda_e = 1, R = 0.5)$ shows a different behavior. As discussed in the last section, the unevenness of the Matern cluster fields with varying cluster sizes can not be directly compared to one another which is confirmed by the results. While the curve almost coincides with the case of $(\lambda_e = 1, R = 1)$ for small user densities, it approaches the case of $(\lambda_e = 0.5, R = 1)$ for larger user densities.

Site/selection diversity gain can as well be stated in terms of transmit power reduction of the mobile stations. Yet, this kind of gain is heavily dependent on the Active Set size

of a single mobile and should be studied separately. This is done in Figure 6, where the transmit power reduction in the Poisson case (see also [3]) and the Matern cluster field ($\lambda_e = 0.5, R = 1$) are depicted and compared for Active Set sizes of 1, 2, and 3.

While the mean additional gain only reaches values from 0.01 to 0.06 dB for small densities it ranges from 0.20 to 0.38 dB for high densities. Comparing the run of the curves with identical AS sizes shows that the additional gain caused by the unevenness of the user distribution can be found for all MSs in the scenario.

These results may seem non-intuitive at first sight. However, the positive effect of uneven user distributions on the site/selection diversity gain can be explained as follows. The higher the level of unevenness of the underlying user distribution, the more will the average traffic load for a single cell change. Here two distinct cases are possible. The first case is that the cell experiences considerably more traffic. This happens if one or more clusters happen to fall within this cell. The second case is that there are no clusters within a cell, such that there is only a very small number of users to be handled by this BS. Both of these cases, however, have a positive effect on the average interference within the cell.

For the second case this is obvious, since if there is only light traffic within a cell, the interference level will be low also. For the second case the result is less obvious. Nevertheless, from looking at Figure 5 we can derive that the maximum soft handover gain reachable increases proportionally to the load of the cell. This is what happens in the second case, where the average load in a cell increases and thus the site/selection diversity gain increases.

Considering the two cases, we can derive that the overall average interference reduction, which is the sum of all the individual gains, adds up to be higher in clustered user environments than for Poisson fields.

5. CONCLUSION AND OUTLOOK

The effect of uneven user distributions on the macro-diversity gain in UMTS networks has been studied. Matern cluster fields were discussed and the pair correlation function was introduced as a way to measure the level of unevenness of the resulting point fields compared to the frequently used spatial homogeneous Poisson process.

A method was described to estimate the pair correlation function of a given cluster point field. In addition, we presented a way to calculate the exact pair correlation function for Matern cluster fields depending on the parent point density and the cluster size.

The influence of these parameter on the level of unevenness was studied for various Matern cluster fields. It was shown that varying the parent point density results in cluster fields that can be directly compared in terms of their unevenness. However, changing the cluster size results in point fields that can not be easily compared to one another.

Simulation were performed in order to study the influence of the unevenness. We proved that the macro-diversity gain proportionally increases with higher levels of unevenness of the underlying point field. This non-intuitive result is caused by the fact that uneven user distributions cause higher variation of the cell load experienced by single BSs. Two cases can be distinguished, that is BSs with higher average load and BSs with considerably lower average load. However, both of these cases were shown to cause an increase of the

site/selection diversity gain.

The results underline the great impact of macro-diversity on the capacity and coverage of UMTS networks, since simulation results performed for user point fields created by the spatial homogeneous Poisson process perform worse than the more realistic cluster fields studied here.

REFERENCES

1. C. C. Chan and S. V. Hanly, Calculating the Outage Probability in a CDMA Network with Spatial Poisson Traffic, *TVT Journal*, Vol. 50, No. 1 (2001) 183-204.
2. N. A. C. Cressie, *Statistics for Spatial Data*, John Wiley & Sons, Inc., (1993), New York.
3. K. Heck, D. Staehle, and K. Leibnitz, Diversity Effects on the Soft Handover Gain in UMTS networks, *Proceedings of the VTC Fall (2002)*, Vancouver, Canada.
4. P. S. Kumar, S. Nanda, and K. M. Rege, Characterization of Capacity Gain due to Macro-diversity in CDMA Systems, *Proc. of the 15th International Teletraffic Congress*, (1997), 1149-1158, Washington, DC.
5. C. Lee and R. Steele, Effect of Soft and Softer Handoffs on CDMA System Capacity, *TVT Journal*, Vol 47, No. 3 (1998), 830-841.
6. A. Morimoto, K. Higuchi, S. Fukumoto, M. Sawahashi, and F. Adachi, Experiments on Inter-Cell Site Diversity Using Two-Step Selection Combining in W-CDMA Reverse Link, *IEICE Trans. Communications*, Vol. E84-B, No. 3 (2001) 435-445.
7. A. Sendonaris and V. Veeravalli, The Capacity-Coverage Tradeoff in CDMA Systems with Soft Handoff, *Proc. Asilomar Conf. Sig. Sys. Comput.*, (1997), Pacific Grove, CA.
8. D. Staehle, K. Leibnitz, K. Heck, B. Schröder, A. Weller, and P. Tran-Gia, Analytical Characterization of the Soft Handover Gain in UMTS, *Proc. of VTC'01 Fall (2001)* Atlantic City, NJ.
9. D. Staehle, K. Leibnitz, K. Heck, B. Schröder, A. Weller and P. Tran-Gia, Approximating the Othercell Interference Distribution in Inhomogeneous UMTS Networks, *Proc. of VTC'02 Spring (2002)* Birmingham, AL.
10. D. Stoyan and H. Stoyan, *Fraktale - Formen - Punktfelder: Methoden der Geometrie-Statistik*, Akademie Verlag (1992) Berlin, Germany.
11. P. Tran-Gia, N. Jain, and K. Leibnitz, Code Division Multiple Access wireless network planning considering clustered spatial customer traffic, *Proc. of the 8th International Telecommunication Network Planning Symposium (1998)* Sorrento, Italy.
12. V. Veeravalli and A. Sendonaris, The Coverage-Capacity Tradeoff in Cellular CDMA Systems, *TVT Journal*, Vol. 48, No. 5.
13. U. Weiss, Designing Macroscopic Diversity Cellular Systems, *Proc. of IEEE VTC (1999)* Houston, TX.